

Isolation and characterization of *Xenopus laevis* homologs of the mouse *inv* gene and functional analysis of the conserved calmodulin binding sites

Yukuto Yasuhiko^{1,*}, Koichiro Shiokawa^{1,*}, Toshio Mochizuki^{2,*}, Makoto Asashima³, Takahiko Yokoyama⁴

¹Department of Biological Sciences, Graduate School of Science, University of Tokyo, 7-3-1 Hongo, Bunkyo-ku, Tokyo 113-0033, Japan; ²Department of Medicine, Kidney Center, Tokyo Women's Medical University, School of Medicine, Japan; ³Department of Life Science, University of Tokyo, 3-8-1 Komaba, Meguro-ku, Tokyo 158-8902, Japan; ⁴Department of Anatomy and Developmental Biology, Tokyo Women's Medical College, 8-1 Kawada-cho, Shinjuku-ku, Tokyo 162-8666, Japan

The homozygous *inv* (*inversion of embryonic turning*) mouse mutant shows situs inversus and polycystic kidney disease, both of which result from the lack of the *inv* gene. Previously, we suggested that *inv* may be important for the left–right axis formation, not only in mice but also in *Xenopus*, and that calmodulin regulates this *inv* protein function. Here, we isolated and characterized two *Xenopus laevis* homologs (*Xinv-1* and *Xinv-2*) of the mouse *inv* gene, and performed functional analysis of the conserved IQ motifs that interact with calmodulin. *Xinv-1* expresses early in development in the same manner as mouse *inv* does. Unexpectedly, a full-length *Xenopus inv* mRNA did not randomize cardiac orientation when injected into *Xenopus* embryos, which is different from mouse *inv* mRNA. Contrary to mouse *inv* mRNA, *Xenopus inv* mRNA with mutated IQ randomized cardiac orientation. The present study indicates that calmodulin binding sites (IQ motifs) are crucial in controlling the biological activity of both mouse and *Xenopus inv* proteins. Although mouse and *Xenopus inv* genes have a quite similar structure, the interaction with calmodulin and IQ motifs of *Xenopus inv* and mouse *inv* proteins may regulate their function in different ways.

Cell Research (2006) 16:337-346. doi:10.1038/sj.cr.7310044; published online 13 April 2006

Keywords: Left–right asymmetry, *inv*, calmodulin, ankyrin, IQ motif, *Xenopus*, calcium

Introduction

Although vertebrates are externally bilaterally sym-

metric, internal organs show a marked left–right (L–R) asymmetry, such as the left-sided presence of stomach and heart and occurrence of more lung lobes on the right side. This L–R asymmetry is genetically determined, and disturbance of the asymmetry often causes serious cardiovascular disease in humans [1, 2]. Recent progress suggested that primary cilia on the primitive node have an important role in the establishment of the L–R asymmetry. Nodal cilia rotate and make a leftward current [3–5]. This leftward flow subsequently induces asymmetrical gene expression such as *nodal* and *lefty*. The mouse mutant called *inv* (*inversion of embryonic turning*) shows a constant reversal of the L–R asymmetry in internal organs and develops cysts of the kidney [6]. In *inv* mutant mouse embryos, the left side expression of *nodal* and *lefty* is inverted [7, 8] and abnormal nodal flow was reported [4, 9], indicating that *inv* acts upstream of *nodal* and *lefty*. The mouse *inv* gene encodes 1062 amino acids containing 15 tandem repeats of

Correspondence: Takahiko Yokoyama

Department of Anatomy, Kyoto Prefecture University of Medicine, 465 Kajicho, Hirokoji-agaru, Kawaramachi-dori, Kamikyo-ku, 602-0841, Japan
Tel: 81-75-251-5303; Fax: 81-75-251-5304;

E-mail: tyoko@koto.kpu-m.ac.jp

*Present addresses: Yukuto Yasuhiko¹, Koichiro Shiokawa², Toshio Mochizuki³

¹Cellular and Molecular Toxicology Division, National Institute of Health Sciences, 1-18-1 Kamiyoga, Setagaya-ku, Tokyo 158-8501, Japan

²Department of Biosciences, School of Science and Engineering, Teikyo University, 1-1 Toyosatodai, Utsunomiya-city, Tochigi prefecture 320-8551, Japan

³Department of Medicine II, Hokkaido University Graduate School of Medicine, Kita 15, Nishi 7, Kita-ku, Sapporo 060-8638, Japan

Received 1 Oct 2005; revised 14 Nov 2005; accepted 6 Dec 2005, published online 13 Apr 2006

the ankyrin motif, two IQ motifs and two nuclear localization signals [10]. In the *inv* mouse, only the first 91 amino acids of the *inv* protein remain, but the regions containing the ankyrin repeats as well as the IQ motifs were deleted [10, 11]. The introduction of *inv* cDNA completely rescued all the *inv* phenotypes, not only situs inversus but also cyst formation of the kidney, indicating that the loss of the *inv* gene caused these two unrelated abnormalities [10]. In humans, a mutation in the *inv* gene is also responsible for human laterality defects [12] and nephronophthisis (NPHP2) [13]. Thus, the *inv* gene is essential in establishing normal L–R asymmetry and kidney development in both mice and humans.

Previously, we reported that the mouse *inv* protein interacts with calmodulin at two sites, and that microinjection of mouse *inv* mRNA into the right blastomere of two-celled *Xenopus* embryos resulted in randomized L–R asymmetry in the orientation of visceral organs [14]. Furthermore, the calmodulin binding motif (the IQ motif) is critical for mouse *inv* mRNA in randomizing cardiac orientation, and Ca²⁺ regulates the interaction between calmodulin and the mouse *inv* protein.

In this study, we isolated two distinct full-length cDNAs for *Xenopus laevis inv* homologs (*Xinv-1* and *Xinv-2*, accession numbers AF321228 and AF321229 respectively), examined their expression and performed functional analysis of the conserved IQ motifs.

Materials and methods

Cloning of *Xenopus inv* homologs

Degenerative oligonucleotides were designed from regions encoding conserved ankyrin repeats of mouse and human *inv* proteins. Total RNAs of adult *Xenopus* kidney and liver were used as a template for cDNA synthesis. These RNAs were reverse-transcribed with Superscript II (Invitrogen, Carlsbad, California), and used as PCR templates. An amplified product was subcloned into the pGEM T-vector (Promega, Madison, WI) and sequenced. The product encoded multiple ankyrin repeats that were 70% identical in amino-acid sequence to mouse *inv* ankyrin repeats 3–10. The fragment was labelled with ³²P-dCTP using an oligoprimering kit (Amersham Pharmacia Biotech, Uppsala Sweden) and used as a probe to screen a *Xenopus* oocyte cDNA library (Clontech ZL5000a, Clontech, Mountain View, CA, USA). The first screening gave us four *inv*-related cDNA fragments. Sequences showed that three of these fragments encoded the same gene and were named *Xinv-1*, and the fourth cDNA was named *Xinv-2*. We screened at least half a million clones at each library screening.

To obtain a full coding sequence of the *Xinv* genes, we screened cDNA libraries, including two oocyte cDNA libraries (Clontech ZL5000a and ZL5001T), the kidney and liver cDNA libraries (Stratagene, La Jolla, CA, USA) and the stage 11.5 embryo cDNA library (a gift from Dr Bruce Blumberg). Rapid Amplification of cDNA Ends (RACE) was also performed to obtain the 3' end of *Xinv-1* using oocyte cDNA as a template.

Northern hybridization and RT-PCR

For Northern analysis, polyA RNAs were purified from total RNAs obtained from oocytes and liver. Five mg of polyA RNAs were electrophoresed and blotted onto nylon membranes (Amersham Pharmacia Biotech). Membranes were hybridized with a ³²P-labelled *Xenopus inv* probe (*Xinv-1*) and washed with 2×SSC, 0.1% SDS at 60 °C and exposed to X-ray film for 1–7 days.

For RT-PCR, RNA was extracted from embryos at various stages by the AGPC method. Reverse transcription was performed using M-MLV reverse transcriptase (Invitrogen) following the manufacturer's protocol. Primers specific to each *Xinv* clone were as follows:

Xinv-1 forward: 5'-GCT GGT GGA AAA GGA GAAAGC TAG AA-3'

Xinv-1 reverse: 5'-CCT ACA TTA CAA CAC TGG AGA GCG CA-3'

Xinv-2 forward: 5'-CCT ACA TTA CAA CAC TGG AGA GCG CA-3'

Xinv-2 reverse: 5'-CTA CAC CAC ACC AAA CGT CAA TTG AAA-3'.

PCR reaction was performed using Ex Taq (Takara, Kyoto).

We amplified β-actin to verify the RT reaction. Primers for β-actin amplification were actinF: 5'-GGA CTT GGC TGG ACG TGA CCT GAC-3', actinR: 5'-CAG ACT CAT CAT ACT CCT GCT TGC TG-3' 18 cycles of PCR were performed.

Whole-mount *in situ* hybridization

The plasmid pYY94 contained 1453 bp of 3' terminal region of *Xinv-1* ORF (open reading frame) in pBluescript SK(-) (Stratagene, La Jolla, CA, USA). The plasmid was linearized at either the *Not* I site (for the antisense probe) or the *Xho* I site (for the sense probe) and subjected to *in vitro* transcription using T7 or T3 polymerase to produce an antisense or sense probe, respectively, in the presence of digoxigenin-modified UTP. Albino *X. laevis* embryos at various stages were fixed in MEMPFA (0.1 M MOPS pH 7.4, 2 mM EGTA, 1mM MgSO₄, 4% paraformaldehyde) and processed for whole mount *in situ* hybridization as described previously [15]. Coloring reaction was performed overnight at 4 °C, then overnight at room temperature using BM purple (Roche Diagnostics, Basel, Switzerland).

DNA construction, site-directed mutagenesis, *in vitro* transcription for mRNA injection and *in vitro* translation

The ORFs of *Xinv-1* and -2 were PCR-amplified and ligated into the transcriptional vector pCS2+ [16] between the *Eco*R I and *Stu* I sites using a ligation kit (Takara). The sequence was confirmed not to have a mutation. For *Xinv-1* transcription, we substituted the T3 promoter for the SP6 promoter of pCS2+. The plasmids, pYY158 (*Xinv-1*) and pYY159 (*Xinv-2*), were linearized at the *Not* I site, and transcribed with T3 RNA polymerase using MEGAscript kit (Ambion).

Mouse *inv* cDNA (pGEM-mINV) [10] was digested with *Eco*R I (Takara) and the 3 kb fragment obtained was ligated into the *Eco*R I site of pCS2+. The resultant plasmid pYY34 was linearized at the *Not* I site and transcribed with SP6 RNA polymerase. Site-directed mutagenesis of *Xenopus inv* IQ motifs was performed using Gene-Editor kit (Promega). The mutated ORFs were subcloned to pCS2+ (modified its promoter from SP6 to T3) and transcribed with T3 RNA polymerase. To obtain GFP mRNA, pbGFP/RN3P [17] was linearized with *Sfi*I and transcribed with T3 RNA polymerase. All

in vitro transcription was performed in the presence of a cap analog (New England Biolabs).

Two cDNA clones, *Xinv-1* and *-2*, were subjected to *in vitro* translation using rabbit reticulocyte lysate (Promega) in the presence of ³⁵S-methionine. Subsequently, lysates were analyzed with SDS-PAGE. The gel was dried and examined by autoradiography.

Yeast two-hybrid assay

The following plasmids were used to examine the interaction with calmodulin in the MATCHMAKER yeast two-hybrid system (Clontech):

- GBT-158 (*Xinv-1* full-length cDNA)
- GBT-182 (IQ1 mutated in *Xinv-1*)
- GBT-183 (IQ2 mutated in *Xinv-1*)
- GBT-184 (IQ1 and IQ2 mutated in *Xinv-1*)

The vector was derived from the pGBT vector (Clontech). Plasmids were introduced into the Y187 yeast strain with pCaM8 that contained the calmodulin gene fused to an activating domain for the yeast two-hybrid assay. Colonies, grown on minimal media lacking tryptophan and leucine, were tested for β-galactosidase activity with a colony-lift filter assay.

Microinjection of synthetic mRNA

Unfertilized eggs of *X. laevis* were manually ovulated from gravid females that had been injected with a human chorionic gonadotropic hormone, gonatropin (Teikoku Zoki, Kawasaki Kanagawa). Eggs were artificially fertilized, dejellied in 2% cysteine-HCl (pH 8.0) and kept in 0.1×Steinberg's solution [18]. The mRNAs to be tested were microinjected at a dosage of 2000 pg/embryo unless otherwise noted, together with GFP mRNA (200 pg/embryo in all the experiments) in 10 nl of distilled water. As injection of 5 ng mRNA/embryo resulted in a frequent occurrence of malformed embryos (abnormal cleavage and gastrulation failure), we decided to inject 2 ng of *inv* mRNAs per embryo. Microinjection was performed at the late two-cell stage or the early four-cell stage. The mRNA solutions were injected into the right or left half of each embryo in the animal hemisphere at the presumptive dorsal and ventral regions. All of the embryos were placed in 1×modified Barth's solution (MBS), containing 3% Ficoll 400 and 50 μg/ml gentamycin during microinjection. Injected embryos were kept in 1×MBS until stage 7 [19], and subsequently transferred into 0.1×Steinberg's solution for further culture. Embryos were kept at 23 °C in 0.1×Steinberg's solution, containing 50 μg/ml gentamycin, before further observations were made. Embryos were cultured until stage 22 [19], and grouped into left-side injected and right-side injected embryos according to the distribution of the GFP signal under a fluorescent microscope (Olympus Model BHS-RFK, with a filter set for FITC observation). At stage 45, embryos were paralyzed with Tricaine (0.1% in 0.1×Steinberg's solution) and the orientations of heart and gut were examined under a dissection microscope. Statistical analyses were performed using a standard χ^2 test, and $p < 0.05$ was considered a significant difference.

Results

Two *Xenopus inv* homologs contain conserved ankyrin repeats and two IQ motifs

Two *Xenopus* cDNA clones, named *Xinv-1* and *-2*, contained an open reading frame (ORF) homologous to mouse

inv, and encode 1007 and 1002 amino acids, respectively (Figure 1A). Both ORFs started with an ATG initiation codon that agrees with the Kozak rule [20], and have an in-frame stop codon in the 3' end. The clones are 89% identical to each other in amino-acid sequence. Nucleotide sequences of ORFs of *Xinv-1* and *Xinv-2* are 58.2% and 57.8% identical to that of the mouse *inv* ORF. At amino-acid level, *Xinv-1* and *Xinv-2* have 50% and 52% overall amino-acid identity to mouse *inv*. Both *Xinv-1* and *Xinv-2* have 15 repeats of the ankyrin motif in the N-terminus (a yellow box in Figure 1A), and two calmodulin-binding IQ motifs, named IQ1 and IQ2 (16 amino-acid residues), that are highly homologous to those of mouse and human *inv* genes. Amino-acid sequences of the ankyrin repeats of *Xinv-1* are 73.4%, 71.8% and 74.5% identical to that of mouse, chick and zebrafish *inv*, respectively. Amino-acid sequences of the ankyrin repeats of *Xinv-2* are 74.7%, 75.5% and 72.7% identical to that of mouse, chick and zebrafish *inv*, respectively. A search in the *X. tropicalis* database identified a sequence that was homologous to *Xinv-1* and *-2*. The sequence encodes 15 repeats of the ankyrin motif and two IQ motifs. The sequence has 83.5% and 83.1% overall amino-acid identity to *Xinv-1* and *-2*, respectively. We could not find other related sequences in mouse, human and *X. tropicalis* databases. IQ1 is just behind the ankyrin repeats, and IQ2 is located near the C-terminus (red boxes in Figure 1A). We also found two basic amino-acid residues, one next to IQ1 and the other at the N-terminal side of IQ2, conserved between mouse and *Xenopus* (blue boxes), which are named Basic Region (BR)-1 and *-2*, respectively. There is a conserved hydrophobic region (designated HR) in the amino-terminal side of BR2 (green box in Figure 1A). Despite the general similarity of the deduced protein structure, *Xinv-1* has only one monopartite (SV40T antigen type) nuclear localization signal (NLS), and *Xinv-2* has no typical NLS, while there are two typical bipartite (nucleoplasmin type) nuclear localization signals (NLS) in mouse *inv* protein (Figure 1B). These structures are well conserved among species (Figure 1B). Figure 2 shows a phylogenetic relationship among mouse, human, chick, zebrafish and *Xenopus (tropicalis)* and two *laevis (inv)* genes.

Xinv-1 is expressed maternally and in early embryos of *Xenopus*

The Northern hybridization analysis detected two signals of *Xinv* mRNA (about 4.4 and 5.8 kb) in the ovary. Only a larger band (about 5.8 kb) was detected in the liver (Figure 3A). As we obtained two *Xinv* cDNAs, we made specific primers in their 3' ends to distinguish *Xinv-1* from *Xinv-2* mRNAs, and examined their expression. The signal for *Xinv-1* was constantly obtained in RNA from the ovary,

A

Xinv1(<i>X. laevis</i>).seq	1	---MSSPPQGSSLASPVQAAAVTGDKTTLLKLIASSPEVIDDEDLGRTPLMYSVLGDR	56
Xinv2(<i>X. laevis</i>).seq	1	---.N...I...R...Q...	56
invs(<i>X. tropicalis</i>).seq	1	---.N...A...G...L...V...	56
inv(<i>M. musculus</i>).seq	1	MNISEDVLST...QH...N...GA...QR...VGNLSALR...K...RF...C...A...	60
invs(<i>H. sapiens</i>).seq	1	MNKSENLFFA...QH...N...GA...QR...VGNLSALK...K...F...C...A...	60
Xinv1(<i>X. laevis</i>).seq	57	RS CABALLKHGAQVNHDPDRSRTALHLAAQTGNHRLKLLSRKADCTHRDLRDIITAVHL	116
Xinv2(<i>X. laevis</i>).seq	57	...K...R...S...R...C...L...	116
invs(<i>X. tropicalis</i>).seq	57	...N...R...S...R...C...L...	116
inv(<i>M. musculus</i>).seq	61	VD...D...A...D...KT...H...R...K...Y...FM...T...R...NWMQK...EEM...PL...	120
invs(<i>H. sapiens</i>).seq	61	LD...D...A...D...KT...H...R...K...Y...FM...T...R...NWMQK...EEM...PL...	120
Xinv1(<i>X. laevis</i>).seq	117	STRHQDTRCLALI LKYTPPGVDAQDRKQTALHWSAYYNRPRHVRLLVRHGSNIGIPDT	176
Xinv2(<i>X. laevis</i>).seq	117	...Q...L...V...V...Q...	176
invs(<i>X. tropicalis</i>).seq	117	...L...V...V...V...	176
inv(<i>M. musculus</i>).seq	121	T...RSPK...L...FMA...E...T...KN...N...E...AK...IK...D...	180
invs(<i>H. sapiens</i>).seq	121	T...RSPK...L...FMA...E...T...KN...N...E...K...IK...D...	180
Xinv1(<i>X. laevis</i>).seq	177	EGKIPLHWAAGHKDPEALTVRCLEEAAPTESLLNWQDVEGRTPHLAVGDGNQEVVRL	236
Xinv2(<i>X. laevis</i>).seq	177	...F...	236
invs(<i>X. tropicalis</i>).seq	177	...V...	236
inv(<i>M. musculus</i>).seq	181	...N...S...VH...I...D...F...A...LT...DV...	240
invs(<i>H. sapiens</i>).seq	181	...N...S...VH...I...D...F...A...VT...DV...	240
Xinv1(<i>X. laevis</i>).seq	237	TSYRCNVAPYDNLFRTPHLHWAALLGYTPINHLLETNNSPKIPSDSQGATPLHYAAQGN	296
Xinv2(<i>X. laevis</i>).seq	237	...H...R...S...I...V...	296
invs(<i>X. tropicalis</i>).seq	237	...V...V...H...R...K...GT...	296
inv(<i>M. musculus</i>).seq	241	...ES...ITS...HAQ...V...R...K...GT...S...	300
invs(<i>H. sapiens</i>).seq	241	...ES...ITS...HAQ...V...R...K...GT...S...	300
Xinv1(<i>X. laevis</i>).seq	297	CPDITRVVLSHISVHDEADLEGRTAFMWAAGKGSDEVVRTMLELDPELEVNRTDKYGGTA	356
Xinv2(<i>X. laevis</i>).seq	297	...P...L...N...K...H...V...	356
invs(<i>X. tropicalis</i>).seq	297	...P...L...H...V...	356
inv(<i>M. musculus</i>).seq	301	FAE...K...F...Q...P...K...DS...S...N...D...L...S...KSDI...MS...	360
invs(<i>H. sapiens</i>).seq	301	FAE...K...F...K...P...K...DS...S...N...D...L...S...KSDI...MA...	360
Xinv1(<i>X. laevis</i>).seq	357	LHAASLSGQITTVRILLENRVQVDAVDMKHTALFRACEMGHREVISLTKGGAKVHLVD	416
Xinv2(<i>X. laevis</i>).seq	357	...A...A...P...A...A...V...	416
invs(<i>X. tropicalis</i>).seq	357	...G...A...P...A...A...V...	416
inv(<i>M. musculus</i>).seq	361	...A...HVS...KL...D...DA...T...P...D...Q...R...D...	420
invs(<i>H. sapiens</i>).seq	361	...A...HVS...KL...N...T...P...D...Q...R...D...	420
Xinv1(<i>X. laevis</i>).seq	417	KDGRSPLHWAALGGNAVYQILLENINPDAQDVEGRTPLQCAAYGGYICGMEVLMENKA	476
Xinv2(<i>X. laevis</i>).seq	417	...V...V...V...V...N...A...	476
invs(<i>X. tropicalis</i>).seq	417	...V...V...V...V...N...A...	476
inv(<i>M. musculus</i>).seq	421	Q...H...L...D...K...NV...A...N...A...N...	480
invs(<i>H. sapiens</i>).seq	421	Q...H...L...D...K...NV...A...N...A...N...	480
Xinv1(<i>X. laevis</i>).seq	477	DPNIQDKVGRALHWSCNNGYLDVAKLLLGYSAFPQMENTEERYTPLDHALGGHQEVI	536
Xinv2(<i>X. laevis</i>).seq	477	...N...V...V...V...	536
invs(<i>X. tropicalis</i>).seq	477	...V...V...V...V...	536
inv(<i>M. musculus</i>).seq	481	...E...I...DFA...N...ERH...	540
invs(<i>H. sapiens</i>).seq	481	...E...I...DFA...N...ERH...	540
Xinv1(<i>X. laevis</i>).seq	537	QFMLEHGALSIAAIQDIAASKIQAVYKGVKVRSAFQRKNLLMKHEQLRKAAAKKREGE	596
Xinv2(<i>X. laevis</i>).seq	537	...P...V...Y...K...RD...D...E...	596
invs(<i>X. tropicalis</i>).seq	537	...P...V...Y...K...RD...D...E...	596
inv(<i>M. musculus</i>).seq	541	...F...Y...K...RD...D...E...	600
invs(<i>H. sapiens</i>).seq	541	...F...Y...K...RD...D...E...	600
Xinv1(<i>X. laevis</i>).seq	597	NRQKGVGQTEGKQKDENHVMRODKSNEHIQNEVMREWYGEETGRAEDRKEEHQEEQN	655
Xinv2(<i>X. laevis</i>).seq	597	...V...K...ADSME...N...Q...IK...VH...Q...AS...N...GK...R...	654
invs(<i>X. tropicalis</i>).seq	597	...H...VR...C...R...LME...N...QQ...T...IVH...H...AV...NS...ECO...VD...K...	655
inv(<i>M. musculus</i>).seq	601	...KR...	604
invs(<i>H. sapiens</i>).seq	601	...KR...	604
Xinv1(<i>X. laevis</i>).seq	656	IEPKQLKHSKHMEQNSKSIANKQKRAGHIQSSPIEHVHTNSIQTRMSPSRISHSPLG	715
Xinv2(<i>X. laevis</i>).seq	655	...L...TNH...Q...RITAQ...S...E...I...T...G...NTQ...	707
invs(<i>X. tropicalis</i>).seq	656	...H...L...PTG...R...TACV...P...NENI...V...I...G...NAQ...S...	712
inv(<i>M. musculus</i>).seq	605	...EAEQQK...QLD...PRSHCSS...APVLP...PSPQNEG...KQDA...	644
invs(<i>H. sapiens</i>).seq	605	...EAEQQK...R...RSPDS...CRPQA...LPCLPS...QDVP...RQSR...	638
Xinv1(<i>X. laevis</i>).seq	716	NETPKMYWDDNPQNTQPRRTSRPQIESPNIIVHRIEDLVOKESRRKSHREERKGSHR	775
Xinv2(<i>X. laevis</i>).seq	708	...I...S...KH...T...H...M...DVV...I...	767
invs(<i>X. tropicalis</i>).seq	713	...IE...N...SHKH...N...I...HRM...DVV...I...K...	772
inv(<i>M. musculus</i>).seq	645	TPSKQPPASHTVQSPDPEHS...LPGRCRGRASQGDSS...DL...GTAS...PSETPIEHCRCG	701
invs(<i>H. sapiens</i>).seq	639	APSKQPPAGNVAQGPPEPRDS...GSPGGSLGGALQKEQHVSSDL...GTNS...RPNETA...EH...KG	698

Xinv1(X.laevis).seq	776 QRASSHRLQASERETAGSVIHGVEVFKKKETKKGRTAAGTSKIRAS--GEAGRLSQSE	833
Xinv2(X.laevis).seq	768 ..Q..DY..HT..K.ASD.A..R.E.G.....V.V.P..E.CCK.GC.K.....	827
invs(X.tropicalis).seq	773 ..E..DN...CV...SN..QT.E.R...G...I.T...TG.C--S.GV.....	830
inv(M.musculus).seq	702 PS..CV.P..SWEGGNSKKNQGTSSVEKRRGETNG..H..CEE.P..SA..QPLCTGS..PAEKG	761
invs(H.sapiens).seq	699 ..S..CV..F..PNEGSDGSRHPPGVPVSEKSRGETAGDE..C..K..KGFVKQPSICIRVAGPDEKG	757
Xinv1(X.laevis).seq	834 KEFSSTGIQGRVDCITSPESETPSRVCRERKMISAKSGORPLTETQ-SPE-----	883
Xinv2(X.laevis).seq	828 ..VSLGI.....P.....T...T.....HKP..G-----	878
invs(X.tropicalis).seq	831 ..SRVV...A...P.....K..SS...KE.....HKP..GMAVQSSSAL	889
inv(M.musculus).seq	762 EDS.PAVASASQDDHPRKPNKRQDRRAARPRGASQKRRT..LRD-RCSPAGSSSRPGSAKGE	820
invs(H.sapiens).seq	758 EDSRRA..ASLPPHDSHWKP..RRHDETPKAKCAPQKRRTQELRGGRCSPAGSSSRPGSARGE	817
Xinv1(X.laevis).seq	884 KAC-----QGSSALKPSLTSHTKQTAIASKCLDSTPSYIGFGEAIKPLTPMGIL	932
Xinv2(X.laevis).seq	879RS....S..P..I...D.....L.....F.....	927
invs(X.tropicalis).seq	890 ..SSMSRHRTQTMAV..S....S.MSR..R..TSD..V..MA.VV...S...S..V..	949
inv(M.musculus).seq	821 V..ADQSSLHRHTPRSKVQTQDKLIGGVSSGLPLSTEASR..GCKQL----YEDICASPET	875
invs(H.sapiens).seq	818 AVHAGQNPPHRTPRKNTVQAKLTGGLYSHLPQSTEE..R..GARRLETSTLSEDFQVSKET	877
Xinv1(X.laevis).seq	933 REGSFSSKNWIDIELIPLEARLQVLEKEKARKOLFRRKAAAVIQAKWRTYCIKSSR	992
Xinv2(X.laevis).seq	928F.....VQ.....R.....V.....V.....C	987
invs(X.tropicalis).seq	950 ...NLT.N...V.....R.....R.....V.S...V..	1009
inv(M.musculus).seq	876 GVAHGPPPG.CMN..H..L.V..Q..LIQKRS...E..R...NK..A..R..S...QL...HLS	935
invs(H.sapiens).seq	878 DPAPGPLSG..SVN..D..L.V..L...TIQKRR..E..RK...NK..A..R..S...QL...HLS	937
Xinv1(X.laevis).seq	993 KTR..ISHLRNRPAMV-----	1007
Xinv2(X.laevis).seq	988RSQ...P.....	1002
invs(X.tropicalis).seq	1010 T...G.AQS...S.....	1024
inv(M.musculus).seq	936 RLL..LKQLGAREVLRCTQVCTALLLQVWRKELELKFPKSISVSRTSKSPKGSATKYAR	995
invs(H.sapiens).seq	938 HL..MKQLGAGDVRWRQESTALLLQVWRKELELKFQTAVSKAPKSPSKGTSKTKSTK	997
Xinv1(X.laevis).seq	1007 -----	1007
Xinv2(X.laevis).seq	1002 -----	1002
invs(X.tropicalis).seq	1024 -----	1024
inv(M.musculus).seq	996 HSVLRQIYGCSQEQKGHHPIKSSKAPAVLHLSVNSLQSIHL-DNSGRSKKFSYNLQPS5	1054
invs(H.sapiens).seq	998 HSVLRQIYGCSHEGKIHHPTRSVKASSVLRVNSVNSLQCIHLLENSGRSKKFSYNLQSAT	1057
Xinv1(X.laevis).seq	1007 -----	1007
Xinv2(X.laevis).seq	1002 -----	1002
invs(X.tropicalis).seq	1024 -----	1024
inv(M.musculus).seq	1055 QSKNKPCL	1062
invs(H.sapiens).seq	1058 QPKNKTPL	1065

B

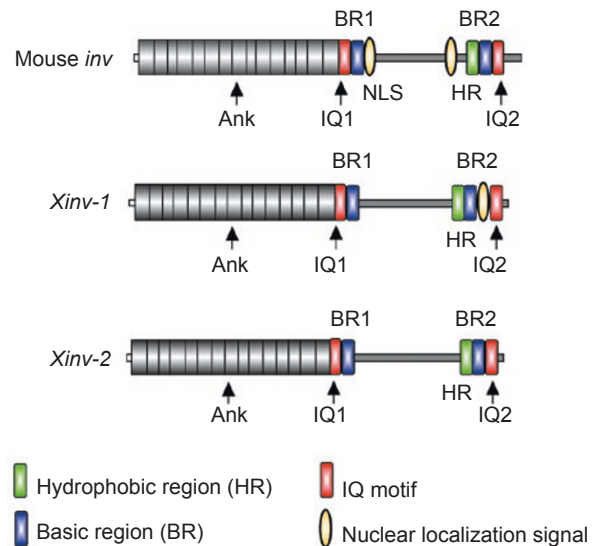


Figure 1 (A) Alignment of putative *Xenopus laevis* inv amino-acid sequences along with mouse, chick (*Gallus gallus*) and zebrafish (*Danio rerio*), and putative *X. tropicalis* inv protein sequences. *Xinv-1*, *Xinv-2*, *X. tropicalis* inv, zebrafish inv, chick inv and mouse inv proteins are 1007, 1002, 1020, 1021, and 1269 and 1138 amino acids, respectively. The conserved motifs are indicated as follows. Yellow boxes: ankyrin repeats, red boxes: IQ motifs, blue boxes: conserved basic regions (BRs), green box: conserved hydrophobic region (HR). IQ motifs and BRs were numbered from the N-terminal (IQ1, 2 and BR1, 2, respectively). (B) Schematic description of the structure of mouse and *Xenopus* inv proteins.

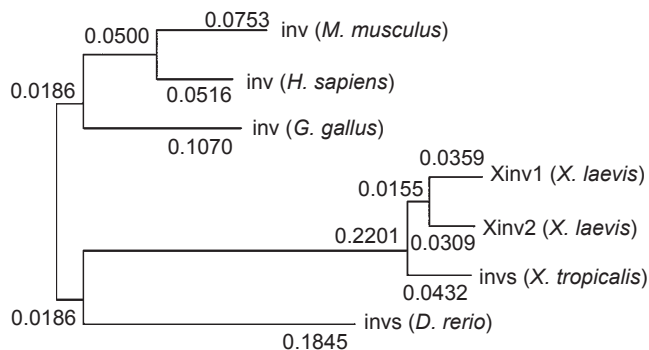


Figure 2 A phylogenetic tree of *inv* related genes. The tree is constructed by the neighbor-joining method [21] using the amino-acids sequences of ankyrin repeat domains. Values indicate expectation of nucleotide substitution on each residue.

cleavage stage embryos through stages 3–27 (Figure 3B). Although the signal for β -actin was detected at 18 PCR cycles, the signal for *Xinv-2* was not detected from the unfertilized egg (ovary) to the hatching stage (St.33), even

at 50 PCR cycles (Figure 3B). The detection of *Xinv* signals in the ovary suggested a possibility that the *inv* message is maternally provided in the egg.

Whole-mount *in situ* hybridization (Figure 3C) showed that the *Xinv* mRNA signal was present in the morula (St. 7) to the tailbud stage. After the neurula stages, *Xinv* signals were detected in the dorsal side of embryos. In the tailbud stage (St. 22), *Xinv* signals were also in the dorsal side with a little anterior bias. No obvious asymmetrical pattern was observed in the examined embryos. Throughout the stages, the signal was not detected using a sense probe.

A single amino-acid substitution of isoleucine to glutamic acid eliminates calmodulin-inv protein interaction

We reported that the region encoding the IQ motifs plays a crucial role in the activity of mouse *inv* mRNA to randomize the L–R asymmetry of *Xenopus* embryos by right-sided mRNA microinjection [14]. Sequence analysis shows that *Xenopus inv* proteins have IQ motifs that are homologous to mouse *inv* protein (Figure 1A and 4A), and yeast two-hybrid assay showed that *Xinv-1* protein also

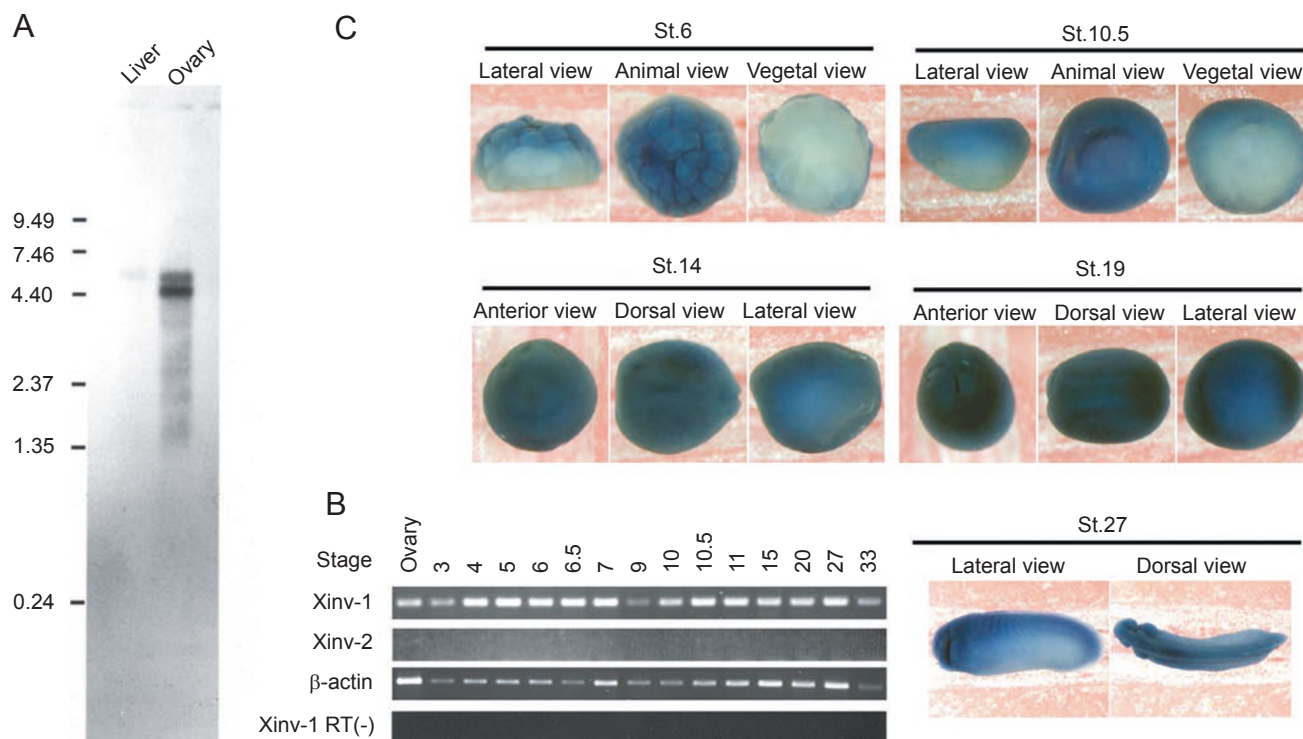


Figure 3 (A) Northern hybridization for *Xenopus inv* cDNA expression. In all, 2 μ g of polyA+RNA is loaded in each lane, and exposed for 7 days at -80°C . A 4.4 kb transcript (arrowhead) was detected in ovary while not in liver. Size markers (in kb) are shown in the left side of the autoradiograph. (B) Temporal expression patterns of *Xenopus inv* examined with RT-PCR. *Xinv-2* is not detected by PCR with up to 50 cycles, while *Xinv-1* is detected at 46 cycles. RT-PCR with β -actin specific primers was carried out in parallel to control the amount of input RNA. RT (-), RT-PCR without reverse transcriptase. Stages are shown over each lane. (C) Expression pattern of *Xinv* from stage 6 to stage 27 shown by whole-mount *in situ* hybridization using digoxigenin-labeled *Xinv-1* cRNA as a probe. No significant unilateral expression of *Xinv* is detected.

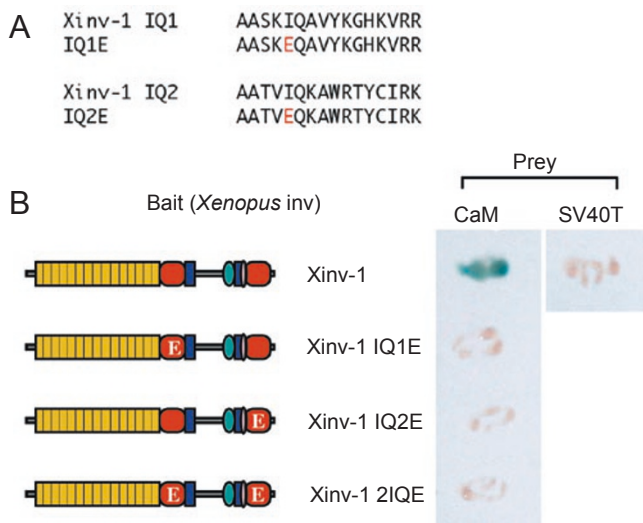


Figure 4 (A) A single amino-acid substitution of isoleucine (I) by glutamic acid (E) eliminates calmodulin–*inv* protein interaction. **(B)** Description of the mutated *Xinv* IQ motifs. Substitution of isoleucine (I) with glutamic acid (E) is indicated in red. IQ motif mutated *Xenopus inv*'s lose calmodulin-binding activity. The interaction between a wild-type *Xinv* protein or mutated *Xinv* proteins and calmodulin or SV40 large T antigen (CaM and SV40T, shown in the upper row as 'prey') was assayed using a yeast two-hybrid system. A schematic description of the constructs indicated in the left column as 'bait'. The white letters 'E' in IQ motifs (depicted as red blocks) represent the amino-acid substitution. In this experiment, wild-type *Xinv* proteins or mutated *Xinv* proteins were used as baits. Blue staining indicates the interaction between bait and prey. Only wild-type *Xinv-1* shows calmodulin binding activity. SV40 large T antigen was a prey as a negative control of the yeast two-hybrid assay, and no interaction was observed.

interacts with calmodulin (Figure 4B).

To verify that *Xenopus inv* protein interacts with calmodulin at the IQ motifs, we performed site-directed mutagenesis at the regions encoding IQ motifs (Figure 4A). We made three mutant constructs of *Xinv-1*, containing a single amino-acid substitution from isoleucine (I) to glutamic acid (E) in one of their IQ motifs or both (Figure 4A). *Xinv-1*/IQ1E, *Xinv-1*/IQ2E and *Xinv-1*/2IQE contain the mutation in IQ1, IQ2 and in both IQ1 and IQ2 regions, respectively (Figure 4B, left column). A full-length ORF of these mutant constructs were cloned into yeast expression vector, and a two-hybrid assay was performed using mouse calmodulin (CaM) as prey. The yeast two-hybrid assay indicated that all these mutants had lost their calmodulin-binding activity (Figure 4B). Interestingly, mutation in either one of the IQ motifs sufficiently eliminated the whole calmodulin binding activity of the *Xinv* protein, indicating that the *Xinv* protein–calmodulin interaction needs two intact IQ motifs.

IQ-mutated but not wild-type *Xinv* mRNA injection reverses cardiac orientation

Microinjection of mouse *inv* mRNA into the right blastomere of two-cell stage *Xenopus* embryos causes randomization of L–R asymmetry and *Xnr-1* expression pattern [14]. To examine whether *Xinv* mRNA has the same effect on L–R asymmetry, we injected synthetic mRNA of *Xinv-1* (total 2 ng per embryo) into one of the blastomeres of two-cell-stage *Xenopus* embryos with GFP mRNA (Figure 5). Unexpectedly, the microinjection of *Xinv-1* mRNAs did not cause an L–R inversion (Figure 6). We performed *in vitro* translation experiment of *Xinv-1* and *Xinv-2* to verify that *Xinv* mRNAs were translated, using rabbit reticulocyte lysate in the presence of ³⁵S-methionine. Resulted lysates were analyzed with SDS-PAGE and autoradiograph, giving signals at the expected molecular size (not shown).

However, when the IQ mutated *Xinv* mRNAs were microinjected into the right blastomere of two-cell stage *Xenopus* embryos, the reversal of cardiac orientation was seen in a significant number of the embryos (Figure 6), though the percentage of cardiac reversals was lower than that caused by mouse *inv*, 18% (*Xinv-1*/2IQE) to 22% (*Xinv-1*/IQ2E). Throughout the experiment, left-sided microinjection had no effect on the cardiac reversal rate when compared with noninjected siblings (not shown).

Discussion

In the present study, we identified two *X. laevis* genes that were homologous to the mouse *inv* gene. The overall similarity between mouse and *Xenopus inv*'s seems to be relatively low, but there are some distinct conserved domains between them: 15 ankyrin repeats, two CaM-binding motifs and NLSs (though NLS is absent in *Xinv-2*). These features are highly conserved among previously identified *inv* homologs of various kinds of vertebrates (mouse, chick and zebrafish). In addition, a search in the *X. tropicalis* database identified a sequence that was more than 80% identical to the two *X. laevis* genes. Although phylogenetic analysis showed that the distance between mouse and *Xenopus inv* genes is larger than that between mouse and zebrafish *inv* genes, this is not significant. Therefore, it is unlikely that the cloned genes are pseudoalleles of the *inv* gene. These results suggest that the genes are *X. laevis inv* genes, and a possibility that their biological functions are shared.

The temporal expression pattern of *Xinv-1* indicated that *Xinv* mRNAs exist maternally and are expressed constantly during embryogenesis, similar to that of mouse *inv* [22]. Whole-mount *in situ* hybridization showed that *Xenopus inv* mRNA expresses evenly in both left and right sides of embryos. These results are also consistent with the previous observation in mouse embryos [10]. Although the

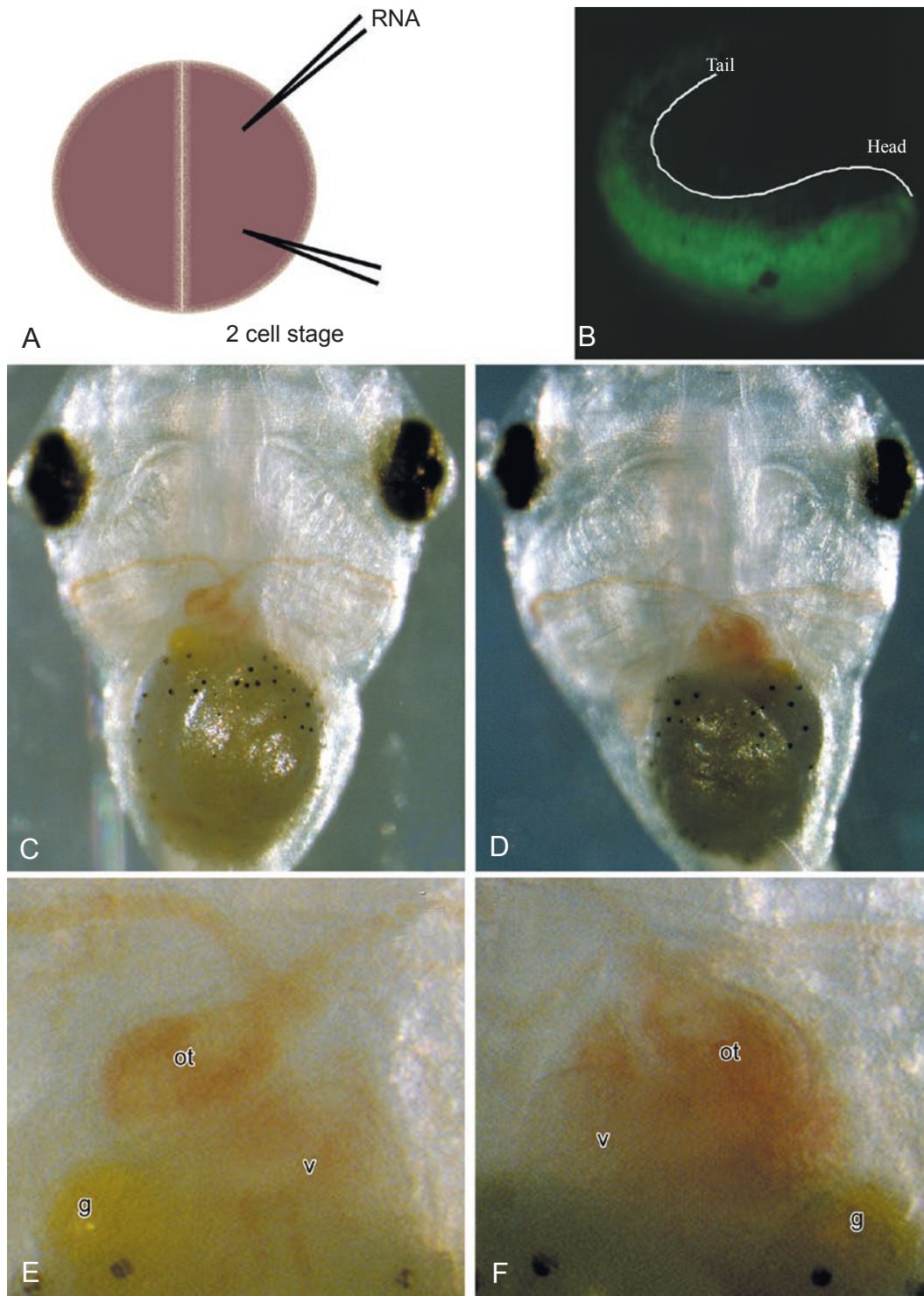


Figure 5 Injection of synthetic mRNAs into the blastomere of the two-cell-stage *Xenopus* embryo and randomization of the L–R asymmetry. **(A)** Microinjection was performed at two-cell or early four-cell stage, and mRNA solutions were injected into the left or right half of the embryos. **(B)** Dorsal view of injected embryo observed under a fluorescent microscopy. GFP fluorescence occurs in the right half of the embryo. The injected embryos were divided into right- and left-injected groups according to the occurrence of GFP fluorescence at St. 23–24. **(C)** A noninjected embryo showing normal visceral L–R asymmetry. **(D)** An example of reversal of L–R asymmetry. **(E)** and **(F)** The outer appearance of normal heart and gall. Abbreviations: ot, outflow tract; v, ventricle; g, gall bladder. Inverted L–R asymmetry of heart and gall in the embryo. Note that the positions of outflow tract and gall bladder are completely inverted.

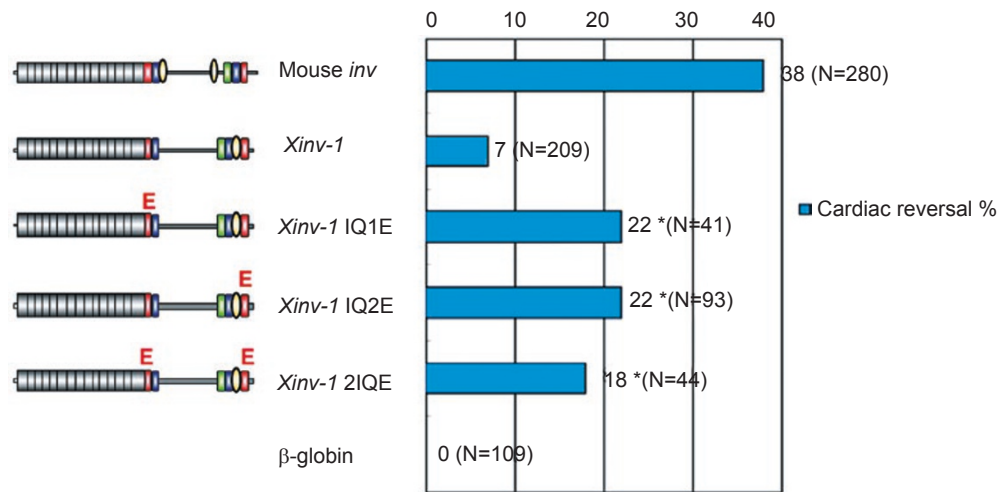


Figure 6 IQ-mutated but not WT *Xinv* mRNA injection reverses cardiac orientation. Cardiac reversal in *Xenopus* embryos injected with the mRNAs coding WT ORF or mutated construct of *Xinv-1*. Schematic description of the constructs indicated in the left lane. The red letters ‘E’ over the IQ motifs (depicted as red blocks) represent the amino-acid substitution. In the right graph, the percentages of embryos with cardiac reversal are shown. All three mutant *Xinv* mRNAs affected L–R asymmetry through the right-sided microinjection of mRNA, while the wild-type *Xinv* mRNAs did not. *Statistically different from that of the group injected with the *Xinv-1*WT RNA into a right blastomere.

present study identified two *Xenopus inv* genes (*Xinv-1* and -2), *Xinv-2* mRNA was not detected by RT-PCR, suggesting that *Xinv-1* is transcribed mainly during *Xenopus* development, and that *Xinv* expression patterns shown by whole-mount *in situ* hybridization (Figure 3) are likely to reflect the distribution of *Xinv-1* mRNA.

A previous study showed that the injection of mouse *inv* mRNA into *Xenopus* two-cell-stage embryos reverses cardiac orientation [14], and suggested that calmodulin signalling was involved in the *inv* pathway for the establishment of L–R asymmetry. Unexpectedly, mRNAs encoding wild-type *Xenopus inv* proteins did not affect cardiac orientation when injected into *Xenopus* two-cell stage embryos. As the N-terminal ankyrin repeats are highly homologous, the difference between mouse and *Xenopus invs* on cardiac inversion is likely to lie in the C-terminal half of *inv* proteins, probably by the interaction between calmodulin and IQ motifs. IQ-mutated *Xinv-1* mRNA randomized cardiac orientation and lost interaction with calmodulin (Figure 6), supporting this idea. The results suggest that the interaction with calmodulin also regulates the *Xenopus inv* function. The mutation in only one of the two IQ motifs eliminated the overall CaM binding activity of *Xinv* protein (Figure 6), suggesting an intramolecular mechanism controlling the interaction between calmodulin and *inv* protein.

Randomization of the L–R asymmetry was induced only when these *inv* mRNAs were injected into the right blastomere, whereas injection into the left blastomere was ineffective. Our results suggest a factor(s) that activates *inv*

protein differently between two blastomeres. The present study suggests that calmodulin is an important factor in the control of *inv* function. Calmodulin is a conserved Ca²⁺-binding protein involved in a variety of cellular calcium-dependent signalling pathways [23–25]. Ca²⁺ regulates the interaction between calmodulin and *inv* protein [14]. As recent studies suggest that there is a difference in Ca²⁺ concentration between the right and left sides in mice [26] and chickens [27], Ca²⁺ might be a candidate as a factor in making the difference in cardiac reversal induced by *inv* mRNA injection between right and left *Xenopus* blastomeres.

Acknowledgments

We thank Dr A Takao for his continuous support and encouragement of this work. We thank Dr H Takeda for his support and encouragement for this work. We thank Dr JB Gurdon for providing pGFP/RN3P. We thank Dr H Saiga, and Dr S Kuraku for helpful discussions. This work was supported by an Open Research Grant from The Japan Research Promotion Society for Cardiovascular Diseases, Grant-in Aid for Scientific Research (C) and Scientific Research on Priority Area (A) to T.Y.

References

- 1 Kosaki K, Casey B. Genetics of human left–right axis malformations. *Semin Cell Dev Biol* 1998; 9:89–99.

- 2 Supp DM, Brueckner M, Potter SS. Handed asymmetry in the mouse: understanding how things go right (or left) by studying how they go wrong. *Semin Cell Dev Biol* 1998; **9**:77-87.
- 3 Nonaka S, Tanaka Y, Okada Y, *et al.* Randomization of left-right asymmetry due to loss of nodal cilia generating leftward flow of extraembryonic fluid in mice lacking KIF3B motor protein. *Cell* 1998; **95**:829-837.
- 4 Okada Y, Nonaka S, Tanaka Y, *et al.* Abnormal nodal flow precedes situs inversus in *iv* and *inv* mice. *Mol Cell* 1999; **4**:459-468.
- 5 Nonaka S, Shiratori H, Saijoh Y, Hamada H. Determination of left-right patterning of the mouse embryo by artificial nodal flow. *Nature* 2002; **418**:96-99.
- 6 Yokoyama T, Copeland NG, Jenkins NA, *et al.* Reversal of left-right asymmetry: a situs inversus mutation. *Science* 1993; **260**:679-682.
- 7 Lowe LA, Supp DM, Sampath K, *et al.* Conserved left-right asymmetry of nodal expression and alterations in murine situs inversus. *Nature* 1996; **381**:158-161.
- 8 Meno C, Saijoh Y, Fujii H, *et al.* Left-right asymmetric expression of the TGF beta-family member *lefty* in mouse embryos. *Nature* 1996; **381**:151-155.
- 9 Okada Y, Takeda S, Tanaka Y, *et al.* Mechanism of nodal flow: a conserved symmetry breaking event in left-right axis determination. *Cell* 2005; **121**:633-644.
- 10 Mochizuki T, Saijoh Y, Tsuchiya K, *et al.* Cloning of *inv*, a gene that controls left/right asymmetry and kidney development. *Nature* 1998; **395**:177-181.
- 11 Morgan D, Turnpenny L, Goodship J, *et al.* *Inversin*, a novel gene in the vertebrate left-right axis pathway, is partially deleted in the *inv* mouse. *Nat Genet* 1998; **20**:149-156.
- 12 Schön P, Tsuchiya K, Lenoir D, *et al.* Identification, genomic organization, chromosomal mapping and mutation analysis of the human *INV* gene, the ortholog of a murine gene implicated in left-right axis development and biliary atresia. *Hum Genet* 2002; **110**:157-165.
- 13 Otto EA, Schermer B, Obara T, *et al.* Mutations in *INVS* encoding *inversin* cause nephronophthisis type 2, linking renal cystic disease to the function of primary cilia and left-right axis determination. *Nat Genet* 2003; **34**:413-420.
- 14 Yasuhiko Y, Imai F, Ookubo K, *et al.* Calmodulin binds to *inv* protein: implication for the regulation of *inv* function. *Dev Growth Differ* 2001; **43**:671-681.
- 15 Harland RM. *In situ* hybridization: an improved whole-mount method for *Xenopus* embryos. *Methods Cell Biol* 1991; **36**:685-695.
- 16 Rupp RA, Snider L, Weintraub H. *Xenopus* embryos regulate the nuclear localization of XMyoD. *Genes Dev* 1994; **8**:1311-1323.
- 17 Zernicka-Goetz M, Pines J, Ryan K, *et al.* An indelible lineage marker for *Xenopus* using a mutated green fluorescent protein. *Development* 1996; **122**:3719-3724.
- 18 Shibata M, Shinga J, Yasuhiko Y, *et al.* Overexpression of S-adenosylmethionine decarboxylase (SAMDC) in early *Xenopus* embryos induces cell dissociation and inhibits transition from the blastula to gastrula stage. *Int J Dev Biol* 1998; **42**:675-686.
- 19 Nieuwkoop PD, Faber J. Normal Table of *Xenopus laevis* (Daudin). New York & London: Garland Publishing Inc 1994:252.
- 20 Kozak M. Point mutations define a sequence flanking the AUG initiator codon that modulates translation by eukaryotic ribosomes. *Cell* 1986; **44**:283-292.
- 21 Saitou N, Nei M. The neighbor-joining method: a new method for reconstructing phylogenetic trees. *Mol Biol Evol* 1987; **4**:406-425.
- 22 Yokoyama T, Shirayoshi Y, Murakami T, Nakatsuji N. Expression of the *inv* gene during development and intracellular localization of the *inv* protein. In: Takao A, Eds. Etiology and Morphogenesis of Congenital heart Disease: Twenty Years of Progress in Genetics and Developmental Biology. Futura Publishing Company: NY, 2000:15-18.
- 23 Crivici A, Ikura M. Molecular and structural basis of target recognition by calmodulin. *Annu Rev Biophys Biomol Struct* 1995; **24**:85-116.
- 24 Chin D, Means AR. Calmodulin: a prototypical calcium sensor. *Trends Cell Biol* 2000; **10**:322-328.
- 25 Jurado LA, Chockalingam PS, Jarrett HW. Apocalmodulin. *Physiol Rev* 1999; **79**:661-682.
- 26 McGrath J, Somlo S, Makova S, *et al.* Two populations of node monocilia initiate left-right asymmetry in the mouse. *Cell* 2003; **114**:61-73.
- 27 Raya A, Kawakami Y, Rodriguez-Esteban C, *et al.* Notch activity acts as a sensor for extracellular calcium during vertebrate left-right determination. *Nature* 2004; **427**:121-128.

Edited by Yun-Bo Shi